DEPARTMENT OF PHYSICS AND GEOPHYSICAL SCIENCES
SCHOOL OF SCIENCES AND HEALTH PROFESSIONS
OLD DOMINION UNIVERSITY
NORFOLK, VIRGINIA

Technical Report PGSTR-AP77-63

THE EVALUATION OF A HgCdTe PHOTOMIXER WITH A TUNABLE DIODE LASER (TDL) AND THE EVALUATION OF TDL'S AS A LOCAL OSCILLATOR IN A HETERODYNE DETECTION SYSTEM

By

Charles N. Harward

E.C. Kindle, Principal Investigator

Final Report
For the period July 1, 1977 - March 31, 1978

Prepared for the
National Aeronautics and Space Administration
Langley Research Center
Hampton, Virginia

Under
Research Grant NSG 1197
Frank Allario, Technical Monitor
Atmospheric Environmental Sciences Division

November 1977

DEPARTMENT OF PHYSICS AND GEOPHYSICAL SCIENCES
SCHOOL OF SCIENCES AND HEALTH PROFESSIONS
OLD DOMINION UNIVERSITY
NORFOLK, VIRGINIA

Technical Report PGSTR AP77-63

THE EVALUATION OF A HgCdTe PHOTOMIXER WITH A TUNABLE DIODE LASER (TDL) AND THE EVALUATION OF TDL'S AS A LOCAL OSCILLATOR IN A HETERODYNE DETECTION SYSTEM

By

Charles N. Harward

Earl C. Kindle, Principal Investigator

Final Report
For the period July 1, 1977 - March 31, 1978

Prepared for the
National Aeronautics and Space Administration
Langley Research Center
Hampton, Virginia 23665

Under
Research Grant NSG 1197
Frank Allario, Technical Monitor
Atmospheric Environmental Sciences Division

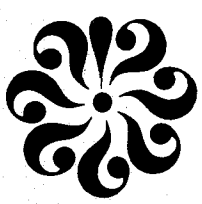

Submitted by the
Old Dominion University Research Foundation
Norfolk, Virginia 23508

November 1977

TABLE OF CONTENTS

LIST OF FIGURES

(cont'd.)

(cont'd.)

(cont'd.)

THE EVALUATION OF A HgCdTe PHOTOMIXER WITH A TUNABLE DIODE LASER (TDL) AND THE EVALUATION OF TDL'S AS A LOCAL OSCILLATOR IN A HETERODYNE DETECTION SYSTEM

By

Charles N. Harward[1]

INTRODUCTION

In recent years, optical heterodyne techniques have been employed to measure different atmospheric constituents (refs. 1 through 5). This technique has proved to be a powerful method because of its high sensitivity and ultrahigh resolution, but the use of fixed frequency CO_2 and CO lasers as local oscillators (LO) limits the usefulness of the technique to chance coincidences between the gas laser frequencies and the characteristic gas absorption lines. Heterodyne systems would be much more versatile if a broadly tunable laser, such as a semiconductor diode laser (TDL), could be used as the LO. There have been only a few papers published (refs. 6, 7, 8) which have shown that a TDL can be used as LO's, but these have shown that TDL lack sufficient power to cause the signal-to-noise ratio to be shot noise limited. The following work was undertaken to fully characterize the heterodyne system with a TDL as the LO.

Spears (ref. 8) in his work on HgCdTe photo diodes, has noted that quantum efficiency and uniformity data obtained from the conventional low-frequency measurements are not necessarily indicative of performance of photomixers at frequencies in the GHz region. Therefore, another part of this research was directed toward mapping out the beat frequency response of the heterodyne system.

---

[1] Research Assistant Professor, Department of Physics and Geophysical Sciences, Old Dominion University, Norfolk, Virginia 23508.

THEORY

Two electromagnetic waves which are moving in the same direction will combine as vectors. Let $\vec{E}_1$ and $\vec{E}_2$ be their respective electric field vectors. The total electric field is given by

$$\vec{E}_T = \vec{E}_1 + \vec{E}_2 \quad . \tag{1}$$

If we assume that the two waves have the same polarization and their values given by $E_1 = E_{10} \cos \omega_1 t$ and $E_2 = E_{20} \cos \omega_2 t$ are the amplitude of each electric field, and ω_1 and ω_2 are the angular frequencies, then

$$E_T = E_{10} \cos \omega_1 t + E_{20} \cos \omega_2 t \quad . \tag{2}$$

If these two waves fall on a detector, and the response S_T of the detector is proportional to the intensity of the radiation or to the square of the electric field, then

$$\begin{aligned} S_T \propto E_t^2 = E_{10}^2 \cos^2 \omega_1 t + E_{20}^2 \cos^2 \omega_2 t \\ + E_{10}E_{20} \cos(\omega_1 - \omega_2)t + E_{10}E_{20} \cos(\omega_1 + \omega_2)t \ . \end{aligned} \tag{3}$$

The detector cannot follow the instantaneous intensity at infrared frequencies; it can only follow the average value of all terms in equation (3), except the third. These averages are $E_{10}^2/2$, $E_{20}^2/2$, and 0 for the first, second, and fourth terms, respectively. The detector can respond to the difference frequency if $\omega_1 - \omega_2$ is within the bandwidth of the detector. Therefore, the response of the detector to the two incident waves is given by

$$S_T = Q\left\{\frac{E_{10}^2}{2} + \frac{E_{20}^2}{2} + E_{10}E_{20} \cos(\omega_1 - \omega_2)t\right\} \tag{4}$$

where Q is the proportionality constant. This signal is made up of a time independent and a time dependent part. The independent part gives rise to a DC component, and the dependent part gives

a component at a frequency $\omega_{IF} = \omega_1 - \omega_2$, the IF frequency. The DC response S_{DC} is given by

$$S_{DC} = \frac{Q}{2} (E_{10}^2 + E_{20}^2) \tag{5}$$

The IF frequency response is given by

$$S_{IF} = Q E_{10} E_{20} \cos \omega_{IF} t \tag{6}$$

The mean square IF response is given by

$$\overline{S_{IF}^2} = Q^2 \frac{E_{10}^2 E_{20}^2}{2} \tag{7}$$

The power in each of the electric fields is P_{10} and P_{20}, and they are related to the electric fields by

$$P_{10} = \frac{E_{10}^2}{2} \tag{8}$$

and

$$P_{20} = \frac{E_{20}^2}{2} \tag{9}$$

Substituting these into equation (7) gives

$$\overline{S_{IF}^2} = 2Q^2 P_{10} P_{20} \tag{10}$$

The proportionality constant Q is given by

$$Q = \frac{\eta e}{h\nu} \tag{11}$$

when the response is given in terms of a current; η is the quantum efficiency, e is the electronic charge, h is Planck's constant, and ν is the optical frequency of the electric field. Therefore, equation (10) is

$$i_{sig}^2 = 2\left(\frac{ne}{h\nu}\right)^2 P_{10}P_{20} \tag{12}$$

where we have assumed that $\nu_{10} \approx \nu_{20}$. If we let $P_{10} >> P_{20}$, then we call the E_{10} electric field the local oscillator (LO) field, and P_{10} the LO power. P_{20} is the signal power. The DC current generated by the LO is

$$I_{LO} = \frac{ne}{h\nu} P_{LO} \tag{13}$$

Thus,

$$i_{sig}^2 = 2\left(\frac{ne}{h\nu}\right) I_{LO} P_{sig} \tag{14}$$

where P_{sig} is the signal power.

In practice, the actual mean square current generated in the IF bandpass is much more complicated than equation (14) suggests. It is given by

$$\begin{aligned} i_{IF}^2 = {} & i_{sl}^2 + i_{bl}^2 + i_{sb}^2 + i_{bb}^2 + i_{bn}^2 + i_{sn}^2 \\ & + i_{ln}^2 + i_{db}^2 + i_{th}^2 + i_{ss}^2 \end{aligned} \tag{15}$$

The term i_{sl} is the heterodyne signal that is to be detected; all the other terms are currents which contribute to unwanted current. The term i_{bl} is the current due to the mixing of the background radiation and the LO radiation. This term would not be included if the sun were used as the signal source. The i_{sb} term is the current due to the mixing of the signal and background radiation. The currents, i_{bb} and i_{ss}, are self-mixing terms; i_{sn}, i_{ln}, i_{bn}, and i_{db} are shot noise currents generated by the signal, LO, background, and the dark current respectively; i_{th} is the noise current generated by thermal processes.

If the radiation from the signal and the background source is chopped and synchronously detected by a lock-in amplifier, there will be several components of the current which contribute to the synchronous signal. The largest component will be the contribution from the beat signal between the signal and the LO. There will be a synchronous component from the beat signal between the background and the LO, and also components due to chopped shot noise from the signal and background. The chopped currents i_{ss}, i_{bb}, and i_{sb} are usually assumed to give a negligible contribution to the synchronous signal. If the sun is used as the signal source, then the chopped shot noise component would be a significant portion of the synchronous signal, especially if the LO power is low or the signal is low. The chopped shot noise from the sun could be reduced if a narrow band pass optical filter centered about the LO frequency were used.

If the sun is used as a source, then the background components will be much smaller than the signal source. The signal-to-noise power ratio will be

$$\frac{S}{N} = \frac{i_{sl}^2}{i_{sn}^2 + i_{dn}^2 + i_{ln}^2 + i_{th}^2} \tag{16}$$

where we have assumed i_{bb} to be small.

The mean squared shot noise due to a DC current is given by

$$i_{sn}^2 = 2eIB \tag{17}$$

where e is the electronic charge, I is the current, and B is the bandwidth of the system. If the current is the result of incident radiation, equation (17) becomes

$$\overline{i_{sn}^2} = 2e^2\eta\, PB/h\nu \tag{18}$$

where the photocurrent equation, equation (13), has been used. The mean squared thermal noise is made up of two parts, the Johnson noise of the mixer itself, and the noise associated with the amplifier. The total thermal noise is given by

$$i_{th}^2 = 4K(T_M + T_{IF}^{eff})B_{IF}G_{deq} \tag{19}$$

where K is Boltzmann's constant, T_M is the physical temperature of the mixer, T_{IF}^{eff} is the effective amplifier temperature which also includes the effects of mixer-amplifier impedance mismatch, B_{IF} is the IF bandwidth, and G_{deq} is the effective shunt conductance of the mixer which contains the IF frequency dependency of the mixer. The frequency response is determined by the finite shunt capacitance, C_d, the series resistance R_s, and shunt conductance G_d. The effective shunt conductance is given by

$$G_{deq} = G_d \left\{ 1 + (\omega^2 G_d / C_d{}^2 R_s) \right\} \tag{20}$$

The effective temperature of the amplifier is given by reference 9

$$T_{IF}^{eff} = T_0(F - 1)\left[\frac{R_{IF}}{4R_0} + \frac{R_0}{4R_{IF}} + \frac{1}{2}\right] \tag{21}$$

where F is the noise figure of the amplifier which is defined at $T_0 = 290°K$, R_{IF} is the input resistance of the amplifier, and R_0 is the resistive component of the output impedance of the photodiode.

Using equations (14), (17), (18) and (19), the signal-to-noise ratio thus becomes

$$\frac{S}{N} = \frac{2(e\eta/h\nu)^2 P_s P_{LO}}{2e^2\eta B_{IF}(P_{LO} + P_s')/h\nu + 4K(T_M + T_A^{eff})BG_{deq} + 2eI_dB} \tag{22}$$

where P_s is the power of the sun or source that has the frequency such that the difference in frequency between the LO and the radiation is in the IF bandwidth. P'_s is all the power of the sun or source which is within the optical bandpass of the system and can excite current carriers within the mixer.

If we express equation (22) in terms of the currents, then it has a somewhat less complicated form. It is given by

$$\frac{S}{N} = \frac{(\eta/h\nu)\ (P_s/B_{IF})}{1 + \dfrac{(I_{dn} + I'_s + I_{th})}{I_{LO}}} \tag{23}$$

where I_{dn} is the dark current, I'_s is the current generated by the solar or source photons that are outside the IF bandpass, but inside the optical filter bandpass, and I_{LO} is the photocurrent generated by the LO. The term I_{th} is given by

$$I_{th} = \frac{2K(T_M + T_A^{eff})G_{deq}}{e} \tag{24}$$

If a thermal source fills the detector's field of view, then the ratio, P_s/B_{IF}, is given by (ref. 10):

$$\frac{P_s}{B_{IF}} = \frac{2h\nu\ T_{op}}{\exp(h\nu/kT) - 1} \tag{25}$$

where the 2 arises from the two sidebands of the LO, and the T_{op} is the transmittance of the system. Thus, equation (23) becomes

$$\frac{S}{N} = \frac{2\eta\ T_{op}}{\left(\exp(h\nu/kT) - 1\right)\left(1 + \dfrac{I_d + I'_s + I_{th}}{I_{LO}}\right)} \tag{26}$$

If the IF system is followed by a lock-in amplifier system with bandwidth B_{LI}, the signal-to-noise ratio is improved by the

factor $(B_{IF}/2B_{LI})^{1/2}$. Where the term T_{op} now includes the factor $1/2$ due to the chopping, the best signal-to-noise ratio is obtained for large LO powers. In this case, the ratio becomes

$$\left(\frac{S}{N}\right)_{SNL} = \frac{2T_{op}\,\eta\,(B_{IF}/2B_{LI})^{1/2}}{\left(\exp(h\nu/kT) - 1\right)} \qquad (27)$$

This is the best signal-to-noise ratio that can be reached by a heterodyne system, and it is known as the shot noise limited signal-to-noise ratio. It should be noted that the signal-to-noise ratio is, in general, a function of the IF frequency due to the frequency dependence of the effective shunt conductance. Thus, for a comparison between the theory and experimental data, the signal-to-noise ratio must be measured at different IF frequencies.

If the source does not fill the heterodyne system's field of view, then the signal-to-noise ratio will be reduced by a factor given by

$$\beta = \frac{A_s}{A_{diff}} \qquad \text{if } A_s \leq A_{diff}$$

$$= 1 \qquad \text{if } A_s > A_{diff} \qquad (28)$$

where A_s is the source area and A_{diff} is the area associated with the diffraction limited field of view, Ω_R.

Siegman (ref. 10) has shown that the effective area, A_{eff}, of the heterodyne system and the field of view of the instrument are related by

$$A_{eff}\,\Omega_R \simeq \lambda^2$$

This was shown as a result of antenna theory. This result leads to a restriction on the heterodyne system. The efficiency of the system cannot be increased by increasing either the field of view or the lens size. The product of the two is a constant for the system. One is increased only at the expense of the other.

Siegman (ref. 10) gave a very good description of the way in which one would determine the heterodyne field of view or, as he calls it, the antenna pattern of optical heterodyne systems. This prescription is as follows: "Consider the complex LO amplitude distribution falling on the photodevice surface (weighted by the quantum efficiency distribution if necessary). Reverse the direction of propagation of this LO distribution and allow the reverse wavefront to propagate back out through any optical elements that an incident signal wave would traverse. The resulting far-field or Fraunhofer diffraction pattern will be the antenna pattern of the optical heterodyne receiver."

EXPERIMENTAL TECHNIQUES AND RESULTS

The research effort has centered around three main activities. The first part dealt with the evaluation of the HgCdTe photovoltaic photomixers and the comparison of the results with theory. The second part dealt with the evaluation of the TDL heterodyne beat frequency characteristics, and the third part dealt with a comparison of the TDL and CO_2 Lasers as local oscillators in a heterodyne system.

I. HgCdTe Photomixer Heterodyne Signal Response and Noise Characteristics

The photomixer that was used in this experiment was supplied by D. L. Spears of MIT's Lincoln Laboratory. The photomixer is shown in figure 1 under ≈100X magnification. The photomixer had a circular shape with a diameter of 300 μm. It was divided into four quadrants. The only quadrant that was active was the one in the upper right-hand corner. The biasing connection and the RF power were taken off the gold bonding tab on the perimeter of this quadrant.

The electronics are shown in figure 2. The biasing supply was connected to the photomixer by a biasing tee as were the IF amplifiers. The bias voltage was adjusted by the potentiometer on the bias supply. The dark current, photocurrent, and bias voltage were read on the bias supply. The IF signal was amplified by the IF amplifier. The signal then passed to a RF 1.2 GHz spectrum analyzer or to the 18 GHz RF detector which converted the RF signal into a DC signal. If the incident radiation were mechanically chopped, the chopped DC signal from the second detector was synchronously detected by an Ithaco Dynatrac 3 Lock-in Amplifier which had the capability of measuring signal and noise simultaneously. These two were then displayed on a stripchart recorder or they were measured and recorded on digital tape for later use.

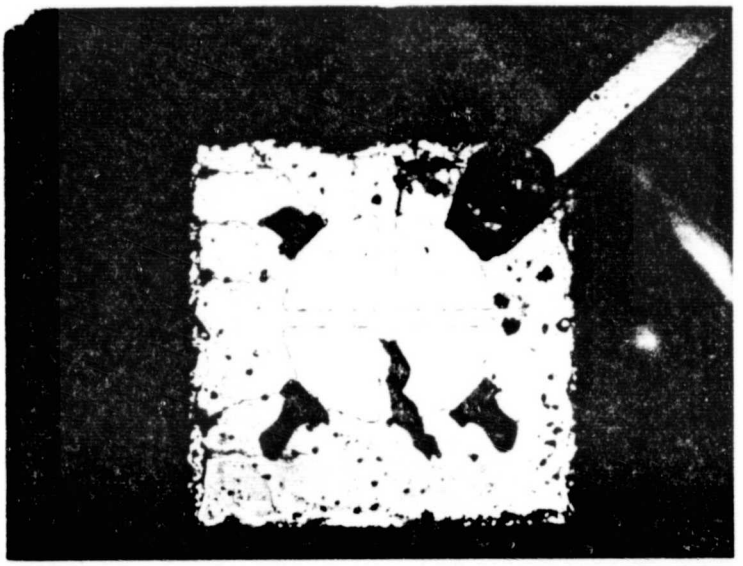

Figure 1. Photograph of HgCdTe photomixer used in the heterodyne system. The photomixer was a 300 μm diameter quadrant detector. It is shown under a X100 magnification. The RF connection and the biasing were made through the gold bonding tab on the perimeter of the quadrant in the upper right-hand corner.

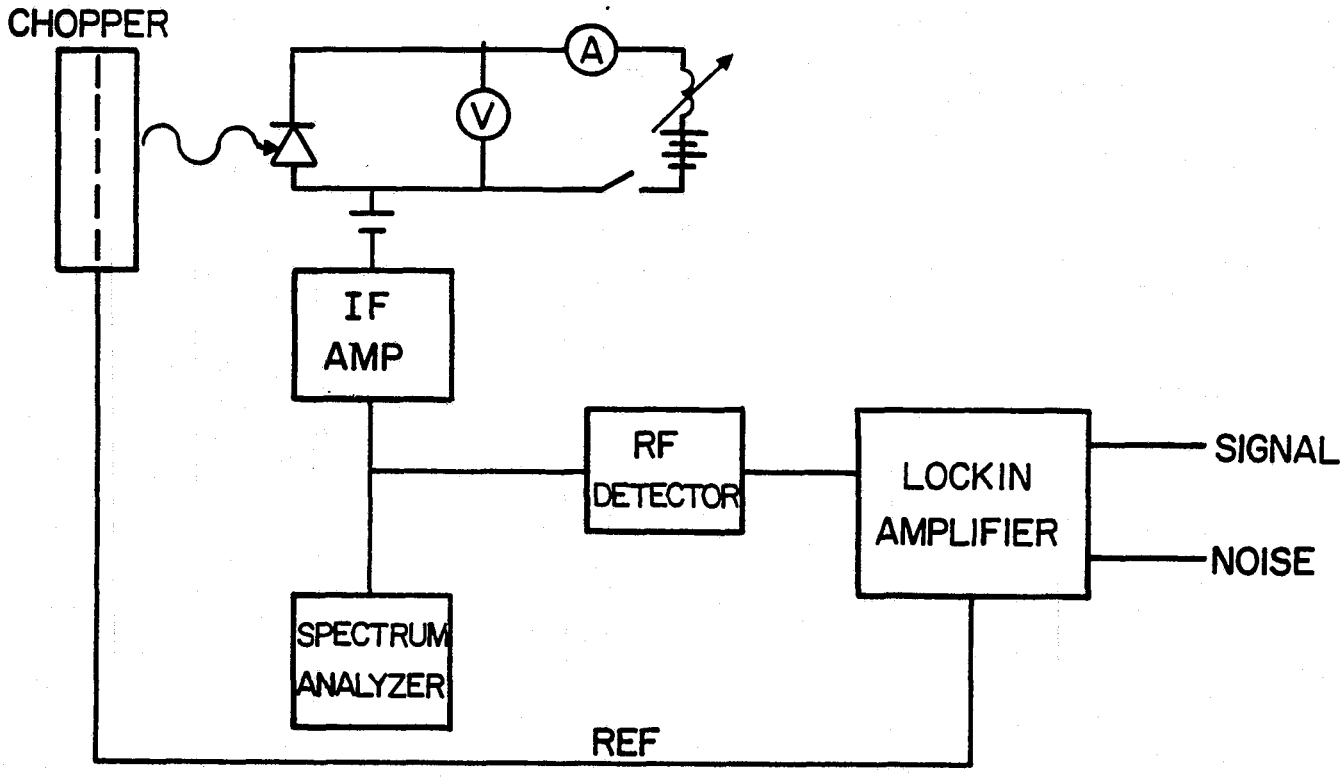

Figure 2. Electronic setup for photomixer bias circuit along with the IF monitoring circuit for the heterodyne signal. This consisted of two IF amplifiers. The first had a 4.2-dB noise figure, while the second had a noise figure of 7.0 dB. Both amplified from 5 to 1500 MHz. The total gain of the two was 70 dB.

The frequency response of the heterodyne system was mapped out by beating a tunable frequency with a fixed frequency CO_2 laser. The tunable frequency was supplied by a TDL. These lasers are indicated in the optical configuration shown in figure 3. The CO_2 laser was a $C^{13}O_2^{16}$ laser with ≈1 watt output power. Because of the high output power of this laser (only ≈ 2 milliwatts were needed), the laser passed through an optical attenuator. To make the CO_2 laser's polarization match the TDL's, the CO_2 radiation's polarization was corrected at the wire screen grid polarizer. The CO_2 laser radiation and the TDL radiation were combined at the beam splitter, which had 32 percent transmittance and 67 percent reflectance. In subsequent measurement, the transmittance and reflectance were found to be highly dependent on the angle of the beam splitter with respect to the optical axis.

Because the TDL radiation was highly divergent, its radiation was collected and collimated by an f/1.5 Ge positive meniscus lens which had been antireflection coated for 10.6-μm radiation. At the beam splitter, part of the TDL radiation was directed toward a 0.5-meter spectrometer which was used to analyze the optical spectra of the TDL. The other part of the TDL radiation passed through the beam splitter and along with the CO_2 radiation, passed to the f/2 Ge antenna lens which focused the combined radiation onto the HgCdTe photomixer.

The I-V characteristics of the photomixer were analyzed with an I-V curve tracer for different CO_2 laser powers incident onto the photomixer. The results of this analysis are shown in figure 4. The voltage axis was horizontal with a 0.1 volt/division (v/div) scale, and the current axis was vertical with a 1.0 mA/div scale. Each of the curves show the I-V characteristic for a known CO_2 power level, except for the straight line which is a calibration curve for a 100 Ω resistor. The lower curve is the I-V curve for no CO_2 laser power. The succeeding curves are for 0.824, 1.37, 1.91, 2.68, and 3.36 mW of incident power. The dynamic resistance of photomixer as determined from the slope of these curves was 79 Ω. The largest change in photo-induced current occurs for a bias of

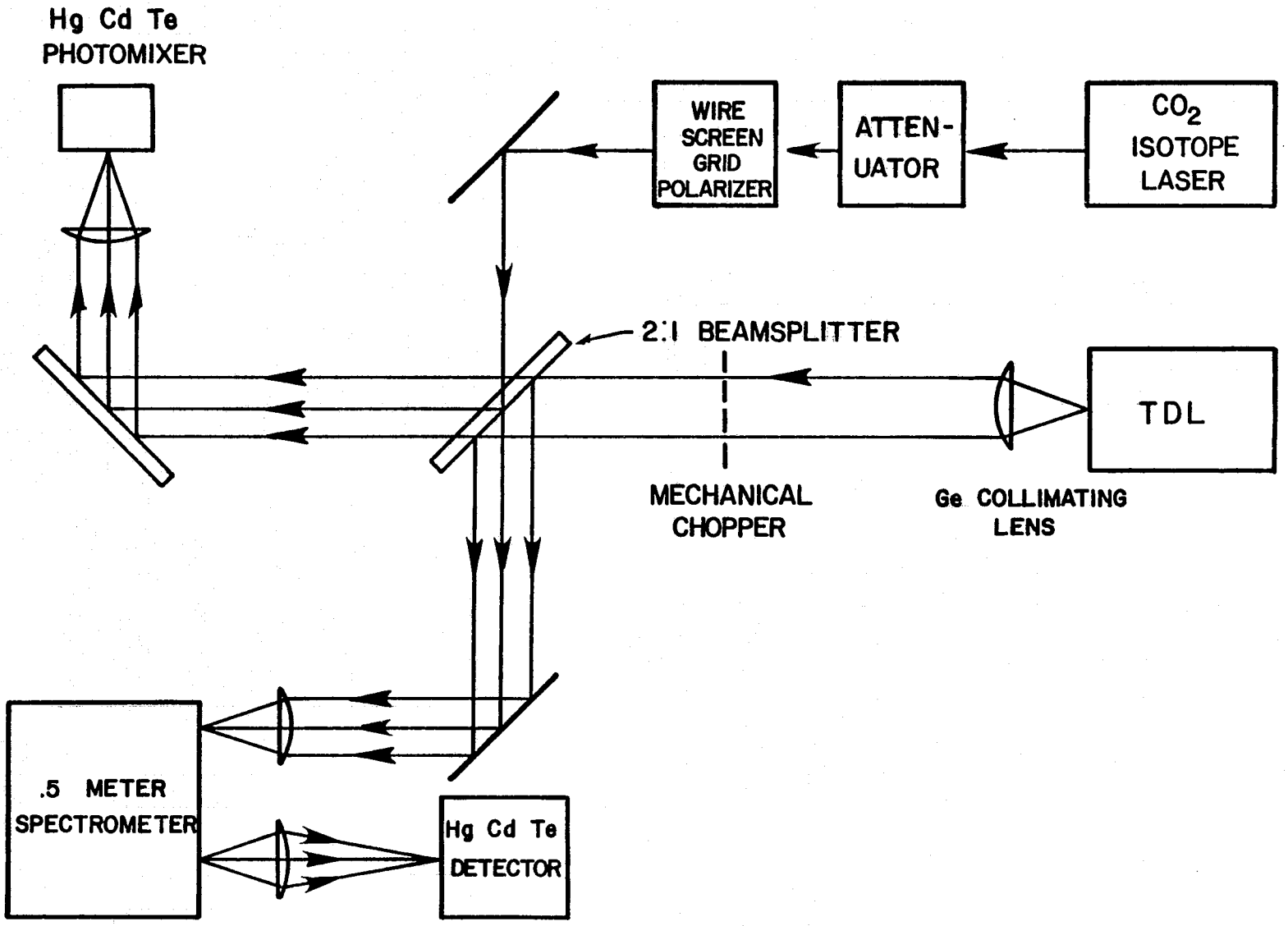

Figure 3. Optical setup of heterodyne system.

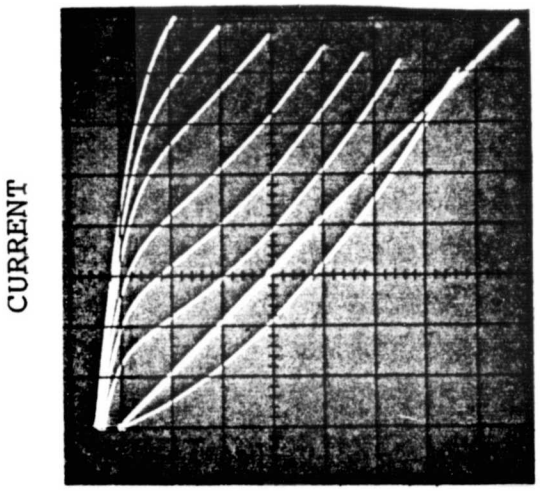

Figure 4. Photograph of the I-V traces of the HgCdTe photomixer for different CO_2 laser power levels. The lower trace was for 0.824, 1.37, 1.91, 2.68, and 3.36 mW laser power. The straight line was generated by a 100 Ω one percent resistor which was used for calibration purposes.

0.4 v. The change in photocurrent at this bias voltage was 4 mA/mW which corresponds to a measured quantum efficiency of ~45 percent. This value was determined at the beginning of the testing; near the end of the testing, the measured quantum efficiency was ~20 percent. The reason for this drop is not evident, but it could have been caused by change in the diffraction limited spot size of the CO_2 laser beam which came about as a result of a reconfiguration of the optical system. This point needs further investigation.

The spot sizes of both the TDL and CO_2 laser are indicated in figure 5. This figure was generated by moving the photomixer across the image formed by the antenna lens. The step size was 9.15 μm. The output of the photomixer was measured by three different methods. The top two curves were generated by direct detection in the photovoltaic mode. The very top was a scan of the CO_2 laser's image, and the next curve was a scan of the image of the TDL. In both of these cases, the full-width half-maximum of the curves was ≈113 μm, which indicated that the spot sizes are smaller than the detector. The third curve from the top was a scan of the heterodyne signal obtained by beating the CO_2 laser and the TDL. The halfwidth in this case was 91 μm. This smaller halfwidth was indicative of the fact that the heterodyne signal was proportional to the product of the CO_2 and the TDL powers, which in this case fall off rapidly away from the center of the image. It should also be noted that the response was not uniform across the detector, which is indicated by the nonsymmetrical nature of the heterodyne curve.

The bottom curve was a scan across the image of the CO_2 laser, but in this case the response was to the RF shot noise generated by the CO_2 laser which was measured at the output of the IF amplifiers. Here the halfwidth was ~165 μm, which was larger than the detector's active area. This result is consistent with the experimental results found by Spears (ref. 8); i.e., the edge of the photomixer gives rise to higher shot noise than in the center.

The RF noise spectrum was determined by connecting the spectrum analyzer to the wideband IF amplifiers. Figure 6 shows the results for two cases. The vertical scale is linear with RF voltage, while the horizontal scale has 100 MHz/div with zero frequency at the far

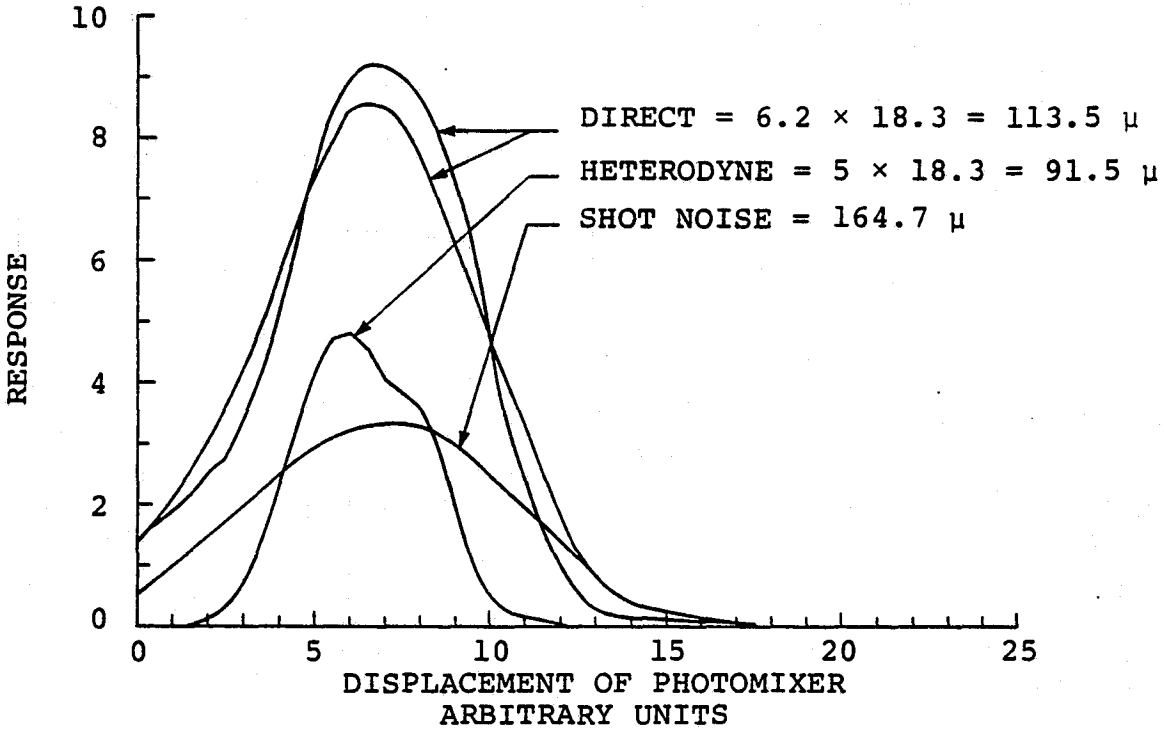

Figure 5. Spot size of the image of the focused laser beam. These curves were generated by moving the photomixer through the image formed by either the TDL or the CO_2 laser. The top two curves were scans of the direct detected image. The third curve down was a scan of the image formed by the TDL and CO_2 lasers using the heterodyne signal. The bottom curve was generated by a scan through the image formed by the CO_2 laser. The response was to the RF shot noise.

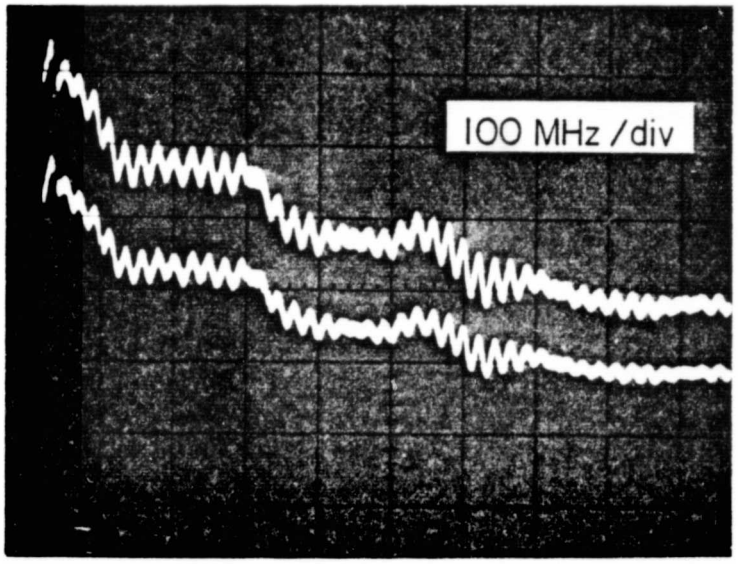

Figure 6. Photograph of the amplifier and shot noise spectra. The two curves in this photograph are the output traces of a spectrum analyzer connected to the IF amplifiers. The bottom trace was for the amplifier noise only, while the top curve was for the amplifier noise plus the shot noise from 2 mA of photo-induced current. The vertical scale was linear, and the horizontal scale was 100 MHz/div.

left. The lower curve shows the noise spectrum of the IF amplifiers. The upper curve shows the noise spectrum with 2.0 mA of photo-induced current and the same bias voltage (0.415 volts) as was the case in the lower curve. The difference in the two curves is due to the shot noise caused by the CO_2 laser. The CO_2 laser was then mechanically chopped, and the vertical output of the spectrum analyzer was fed into a lock-in amplifier where the chopped shot noise was synchronously detected. When the spectrum analyzer was scanned, the shot noise spectrum was mapped out. This is shown in figure 7. The IF amplifiers have a bandpass from 5.0 MHz to 1600 MHz. The low value of the noise at start and end of the scan was a result of the bandpass of the amplifier. The low value at 1450 MHz was an artifact of the spectrum analyzer. The 3.0 dB rolloff point was approximately 1000 MHz. This was indicative of the RC rolloff of the photomizer due to its capacitance and resistance.

The response of the photomixer to a heterodyne beat signal is shown in figure 8. This figure was generated by tuning the TDL to a mode that was within ±1800 MHz of the CO_2 laser which was used as the LO in this experiment. The CO_2 laser was tuned to the P(28) line in the $10°0 - (10°0,02°0)_I$ band of $C^{13}O_2^{16}$. As the current through the TDL was changed by 18 mA, the TDL varied from -1800 MHz below the LO frequency to +1800 MHz above the LO frequency.

The TDL radiation was mechanically chopped before entering the beam splitter in figure 3, and the output of the RF detector was connected to the lock-in amplifier. When the TDL was scanned ±1800 MHz around the LO, the output of the lock-in mapped out the heterodyne response of the system as a function of IF frequency. Figure 8 is one such scan of the heterodyne system response to the different beat signals. The vertical axis has arbitrary units, while the horizontal has units of frequency which were marked off by observing the beat signal on the spectrum analyzer. The cutoff at the extremities of the scan was caused by the 1600 MHz cutoff frequency of the IF amplifier. The amplifier does not transmit a beat signal from -5.0 to +5.0 MHz. The failure of the dip to go to zero indicates a finite line width for the TDL on the order of 10 MHz in this case. The shape of the beat signal on the spectrum analyzer indicated this as well.

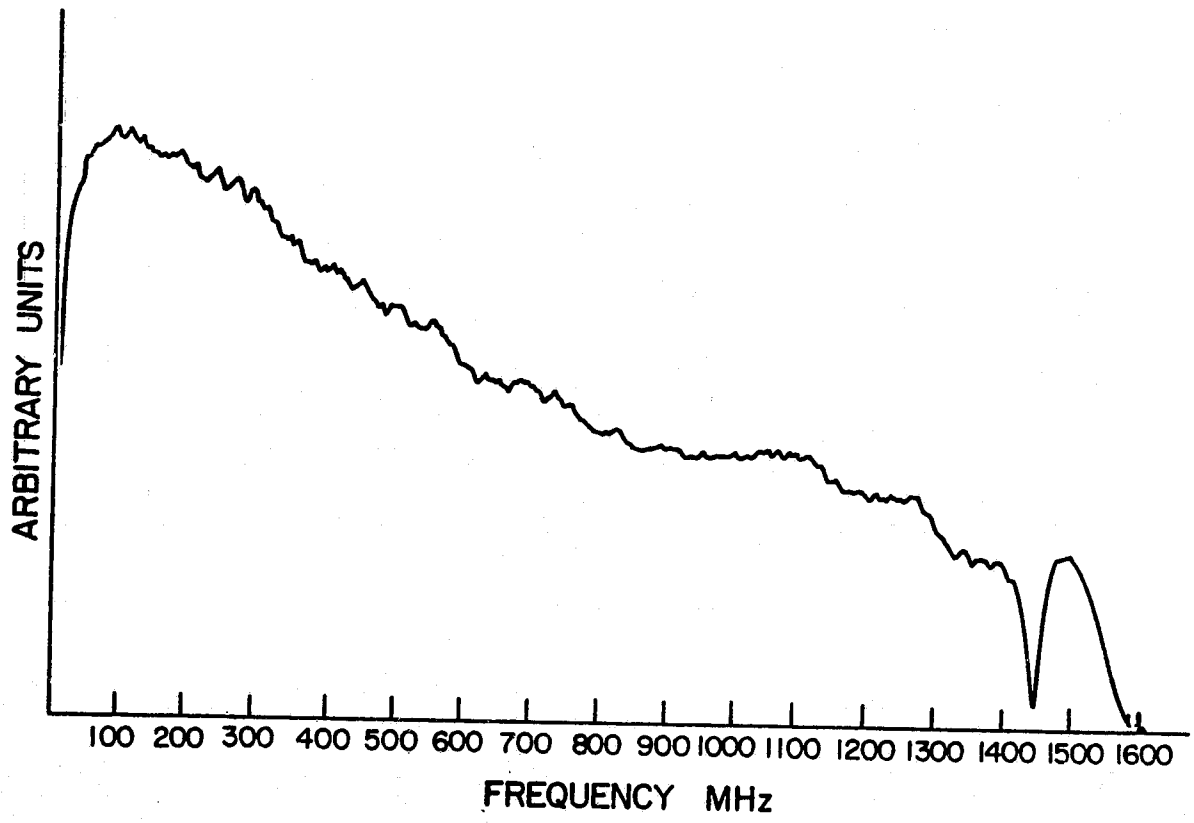

Figure 7. Shot noise spectrum. The shot noise spectrum was determined by slowly scanning the spectrum analyzer over the shot noise induced by a chopped CO_2 laser. A lock-in amplifier was connected to the vertical output of the analyzer, and the chopped signal was synchronously detected as the spectrum was scanned.

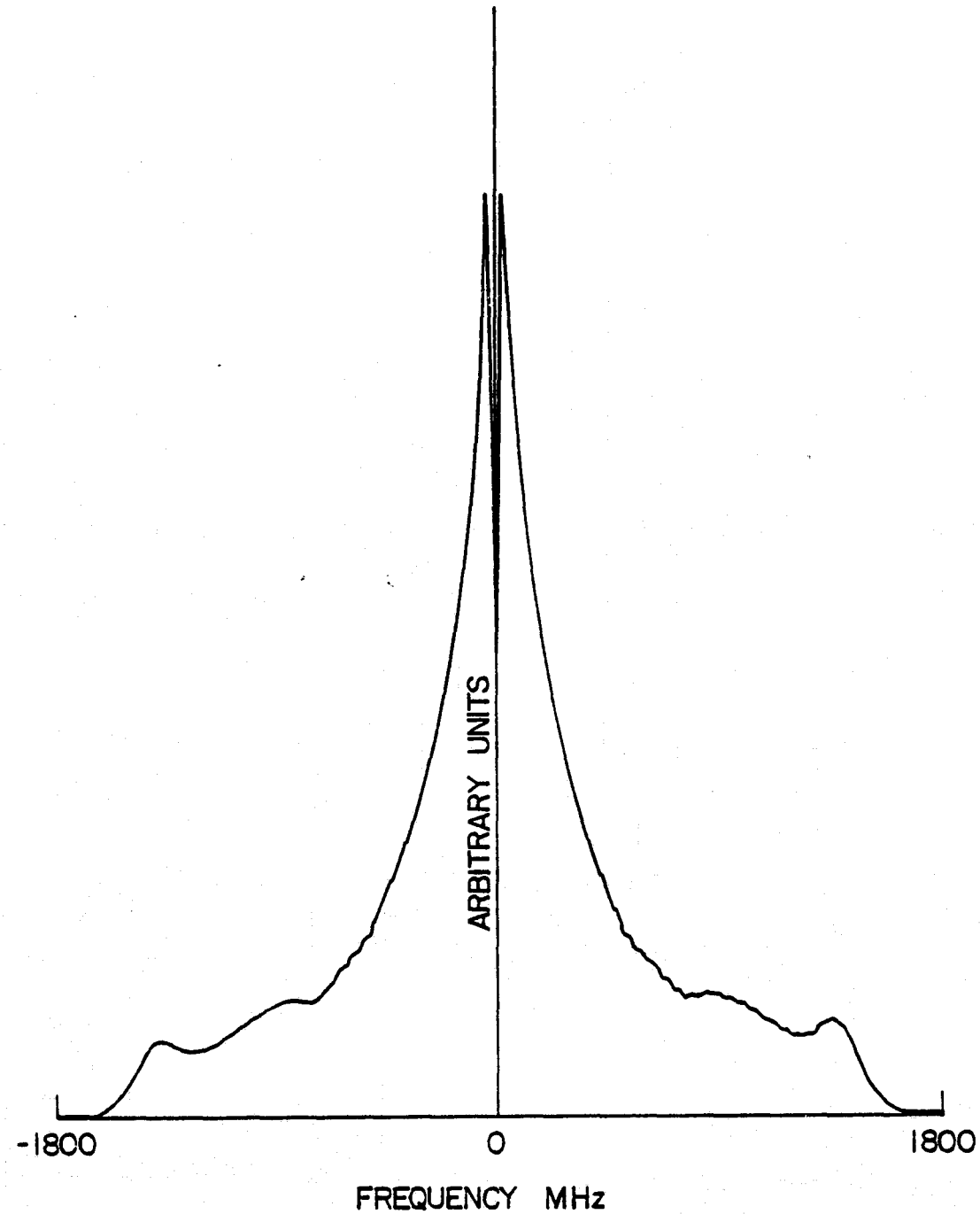

Figure 8. Photomixer heterodyne response. The heterodyne response was mapped out by beating the TDL with the CO_2 laser. The response curve was obtained by scanning the TDL from one side of the CO_2 laser line to the other while recording the heterodyne signal.

The extremely sharp rolloff of the system's heterodyne response is evident from this figure. The 3 dB points are at ±200 MHz for this figure. The TDL mode used to generate the beat signal was so strong that the beat signal was actually saturating the RF detector which caused the peak values to be suppressed. Thus, the rolloff was much more pronounced than indicated in this figure. Attenuation of the TDL radiation caused the rolloff to be much sharper. This effect is shown in figure 9. Here the TDL radiation was attenuated to the point where the RF detector was not being driven to saturation. Only a single sideband is shown in this figure. The image of this sideband followed the same shape. There are two different heterodyne response scans in this figure. The first scan was made at a TDL power level that did not saturate the RF detector. In the second scan, the TDL power was reduced by a factor of 100. The lock-in amplifier gain was then increased by this same factor so that the shape of the two response scans could be compared directly. It is evident that reduced power level scan had a lower signal-to-noise ratio, but the shape of the two curves were identical. But the shape differed from that shown in the previous figure. The 3-dB rolloff in figure 9 is 100 MHz compared to 200 in figure 8. The RF detector saturation caused the rolloff to be increased by a factor of two. Once the TDL power level was reduced so that the RF detector was not saturated, the shape of the heterodyne response curve was independent of the TDL power level.

The independence of the shape of the heterodyne response on LO power was shown by scanning the TDL across the LO line for several different LO power levels. This is shown in figure 10. The response curves for the different power levels are displayed in this figure normalized to the peak response of each of the curves; the vertical scale was logarithmic. The agreement between them was quite good as the power level of the LO was varied from 1.8 mW down to 0.2 mW. The relative response was within 1.0 dB at each of the beat frequencies. However, the three dB points varied from 150 to 280 MHz for the set of curves. This is probably not significant because care was not taken to keep the signal level sufficiently low so as not to saturate the RF detector.

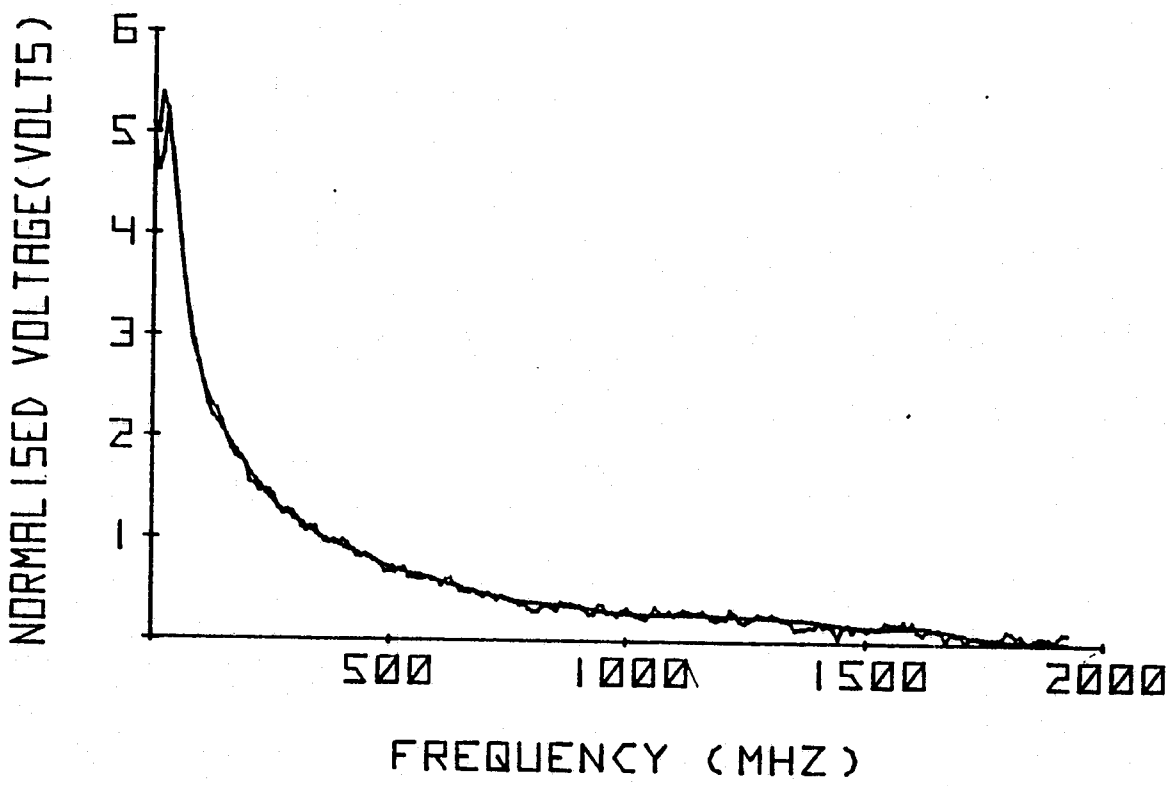

Figure 9. Photomixer heterodyne response. These two curves were obtained in the same manner as figure 8. The power level of the TDL differed by a factor of 100 in the 2 curves. The gain in the case of the lower power was increased by 100 in order to normalize the 2 curves for comparison.

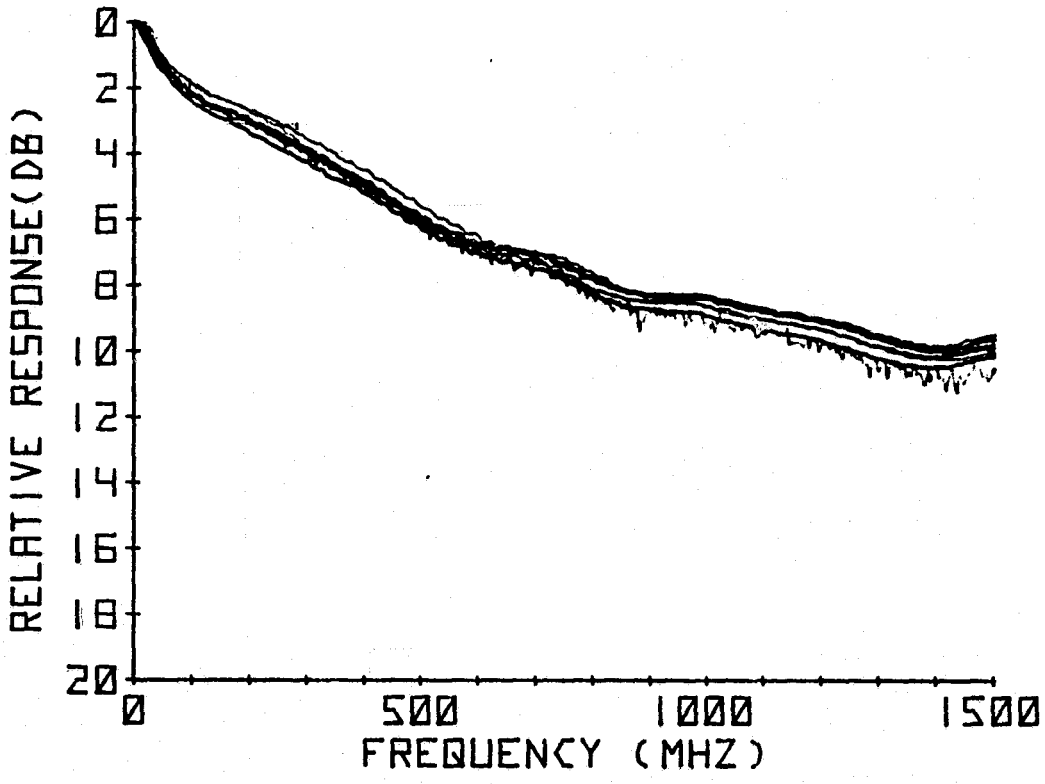

Figure 10. Photomixer heterodyne response as a function of LO power. These curves were obtained in the same way as figures 8 and 9. In this case, the power level of the CO_2 laser was varied from 0.2 to 1.8 mW. The different curves were normalized to the peak response of the curve in order to compare the curves. The curves are plotted with a log scale on the vertical axis.

The dependence of the photoinduced current on LO power is shown in figure 11. During the measurement the bias was kept at a constant 0.40 volts. The linear power dependence of the photocurrent is shown in this figure. The least squares fitted slope of the curve was 1.92 mA/mW, which gave a quantum efficiency of 21 percent.

Figure 12 shows the noise on the output of the lock-in amplifier which was connected to the RF detector. The bandpass of the lock-in amplifier was 9.92 Hz. The noise increases from 7.0 μv to 37 μv as the LO power increases from 0 to 1.7 mW.

The signal-to-noise ratio for the LO beating against a 1500°C black body is shown in figure 13 as a function of the LO power. The ratio increased as the LO power up to about 1.0 mW where the ratio became constant. This was the shot noise limit. Subsequent measurements were made with this photomixer in an optimized system. The 1 mW LO was beat against a 1000°C black body. The signal-to-noise ratio obtained experimentally was 327 with a 312-Hz bandpass on the lock-in amplifier. The ideal signal-to-noise ratio was 1852 for the shot noise limited case. When the other noise terms are included, the signal-to-noise ratio was 576 with an IF bandwidth of 1000 MHz. This bandwidth was the one determined from the shot noise measurements in figure 7. This signal-to-noise ratio was only 1.76 larger than the experimentally determined ratio. If we used a smaller bandwidth as indicated by the system response curve obtained with the TDL, then the agreement would be better. In fact, an IF bandwidth of 322 MHz would give exact agreement between theory and experiment.

In subsequent measurements on another HgCdTe photomixer with a shot noise bandwidth in excess of 1500 MHz, the signal-to-noise ratio showed the same kind of behavior as shown in figure 13. Figure 14 shows the signal-to-noise ratio for this photomixer. The amplifiers were the same as used previously. The quantum efficiency was 0.45, the lock-in amplifier bandwidth was 3 Hz, and the black body temperature was 601°K. For this set of operating conditions, the ideal signal-to-noise ratio was 280. The noise degraded ratio was 89, and the experimental ratio was

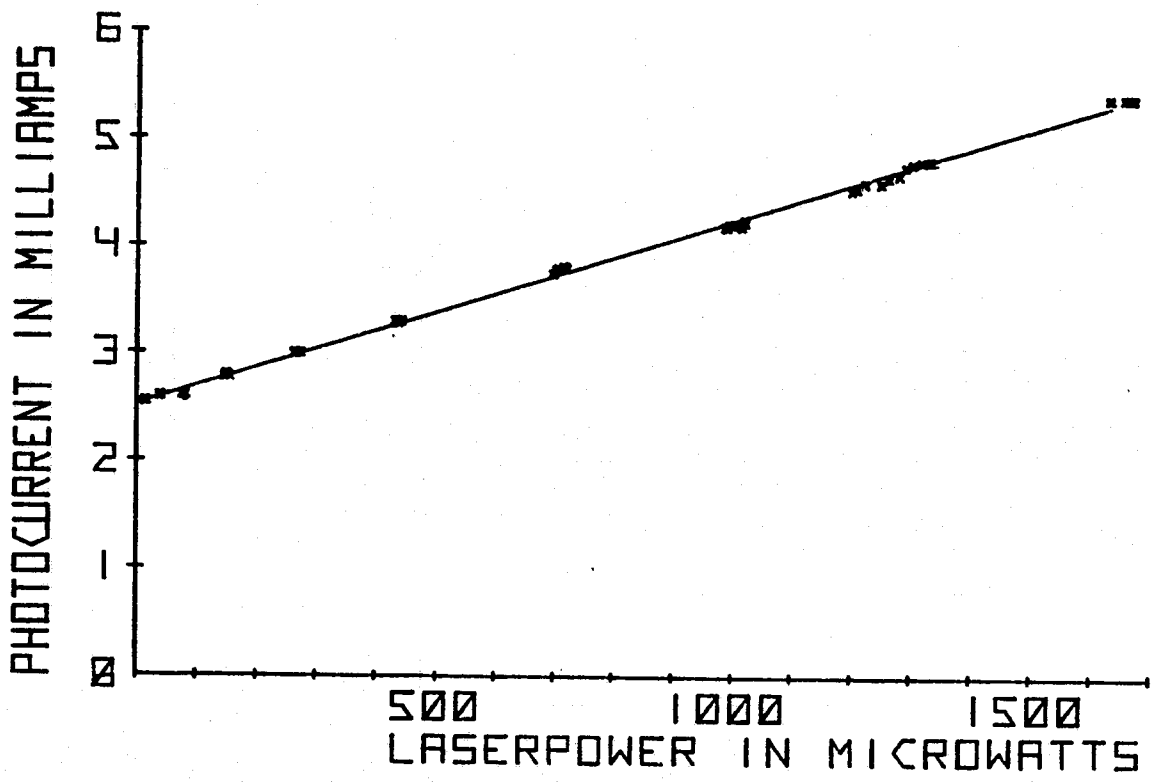

Figure 11. CO_2 laser-induced photocurrent response.

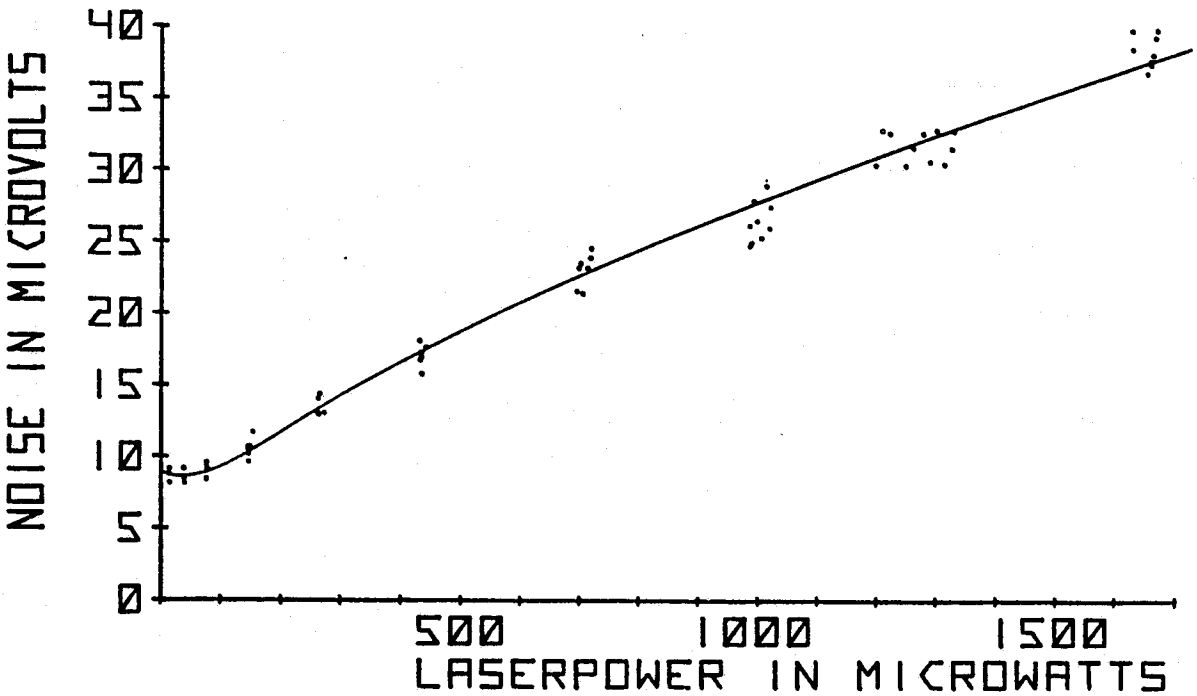

Figure 12. Heterodyne system noise measurements. This curve was obtained by measuring the noise on the heterodyne signal from beating a CO_2 laser against a 1500°C black body with a 9.92 Hz lock-in amplifier bandwidth.

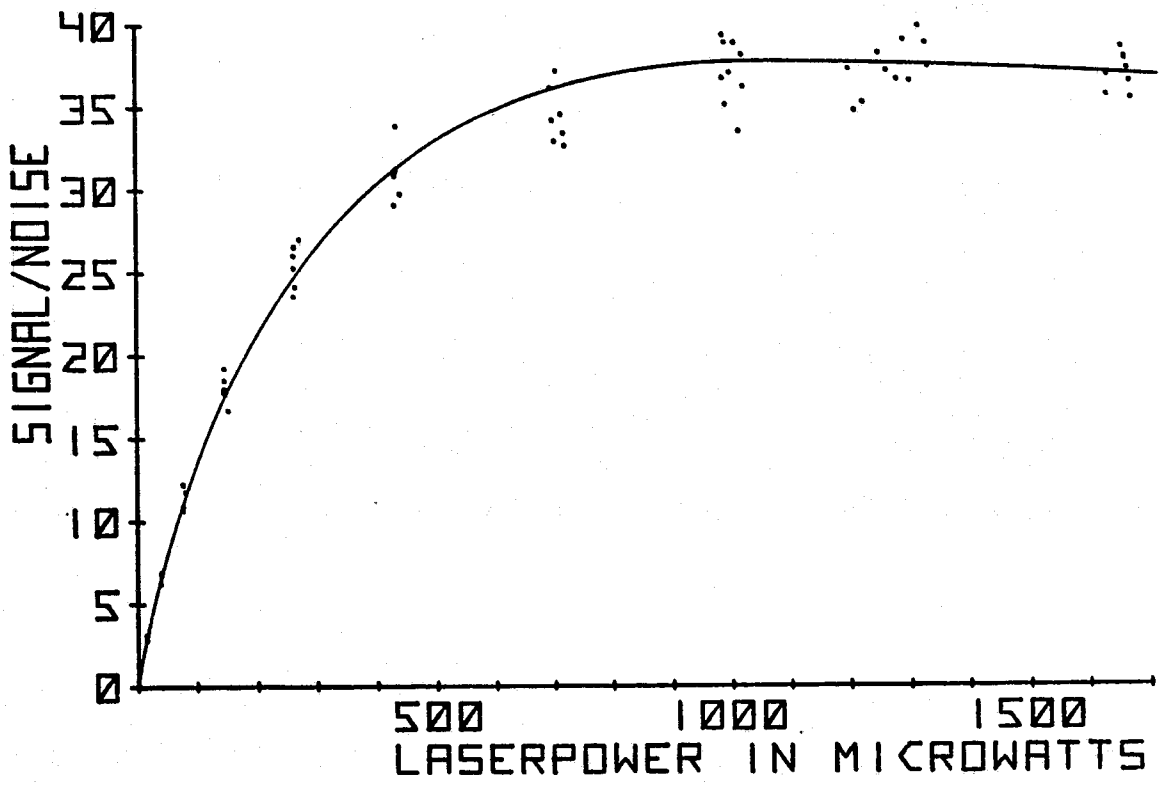

Figure 13. Signal-to-noise ratio. The signal-to-noise ratio was obtained by measuring the signal and noise on the heterodyne signal obtained by beating a CO_2 laser with a 1300°C black body.

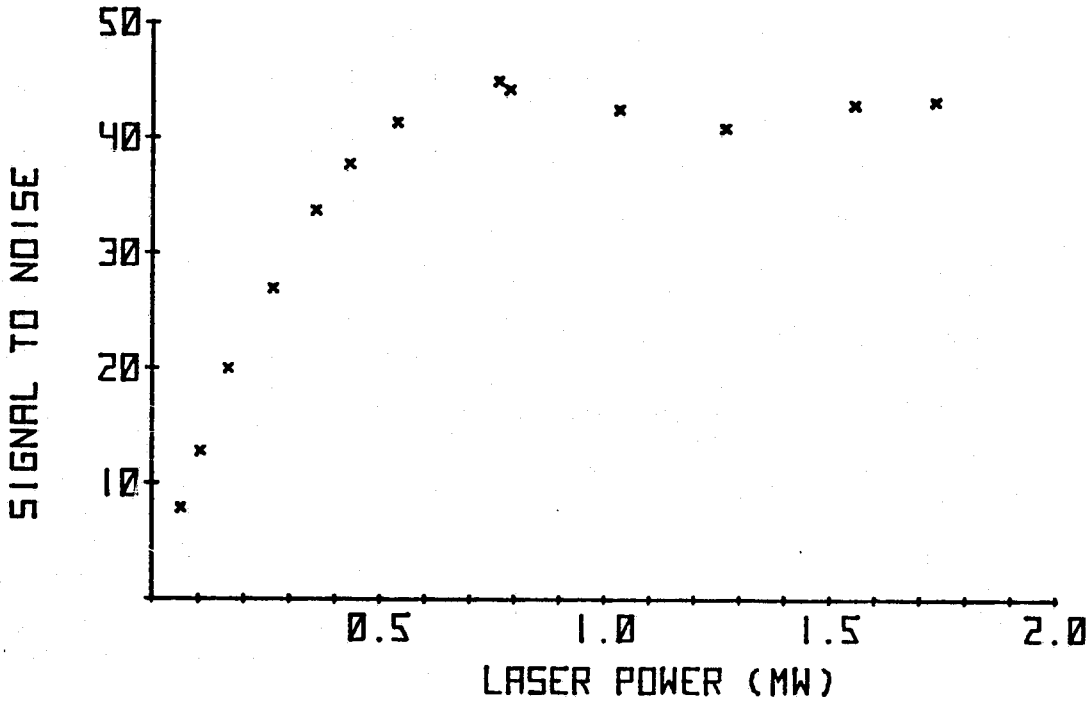

Figure 14. Signal-to-noise ratio. The signal-to-noise ratio was obtained as in figure 13, but a different photomixer was used. The black body temperature was 601°K. The lock-in amplifier bandwidth was 3 Hz.

45. Thus the experimental ratio was a factor of 2 smaller than the theoretical value. If the bandwidth of the system was reduced from the assumed 1500 MHz to 383 MHz, then the experimental and theoretical signal-to-noise ratios would be in exact agreement. This size bandwidth was indicated from measurement of the frequency response of the heterodyne system.

The most important conclusion that can be drawn from the TDL measurement of the heterodyne system's frequency response and the signal-to-noise ratio measurements is that the heterodyne system's frequency response falls off at a much faster rate than is indicated by theoretical considerations.

II. Tunable Diode Laser Evaluation

The TDL was used in Part I as a probe laser operating in a spectral region near the CO_2 LO. The TDL was used to map out the heterodyne response of the photomixer without regard to the properties of the TDL. In this section the beat signal properties will be detailed as will other properties which affect the use of the TDL as the LO in a heterodyne system.

Figure 15 shows a photograph of the beat signal as displayed on the spectrum analyzer with a linear vertical scale and a horizontal scale of 50 MHz/div. The beat signal indicated that the TDL halfwidth was 40 MHz which was typical of the TDL halfwidth seen in this study, although halfwidths as low as 10 MHz and as high as 300 MHz were observed. The large halfwidth occurred when the temperature and current conditions were near the operating threshold of the TDL. The narrower halfwidth occurred when the power of the TDL was quite high. This type of behavior was to be expected. When the TDL was operating near threshold, the radiation field in the TDL was not very coherent. The emitted radiation will be less coherent than the higher power case, hence the line width will be broader. As the TDL operates with higher power, the radiation field inside the TDL has a high degree of coherence and thus a narrow line width.

The output of the TDL is usually multimoded. At times, several longitudinal modes lase as the same time, and these

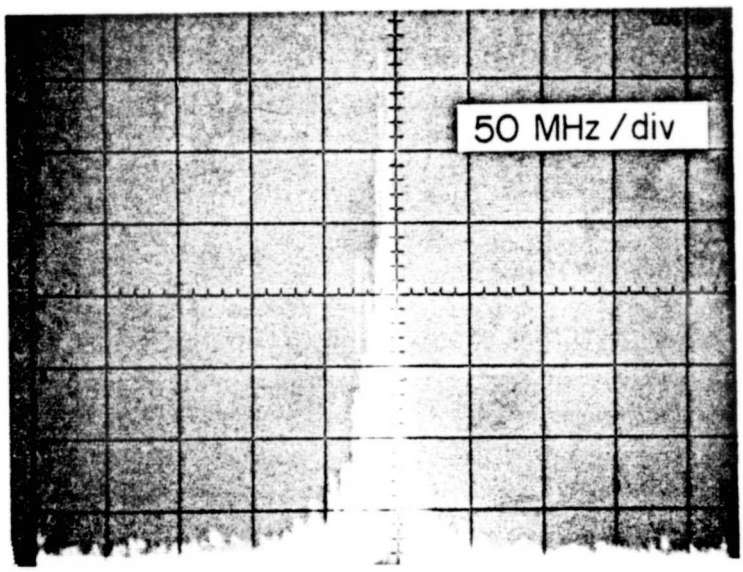

Figure 15. Spectral analysis of the beat signal. This photograph was taken of the trace of a spectrum analyzer scan of the beat signal obtained from beating a TDL with a CO_2 laser. Both scales are linear.

are joined by off-axis modes which may be at frequencies that are very close to one another. The presence of the off-axis modes is possibly shown in the sequence of photographs in figure 16. These photographs show the beat signals obtained by beating the TDL with the CO_2 laser as the LO. Several different spikes appear in the beat signal. The frequency of these spikes is somewhat variable in time. Each of the photographs was taken with the current and temperature conditions held constant. The only change that was made was the placement of an 8-mm aperture in front of the collection lens of the TDL for figures 16a, 16b, and 16c, and this aperture movement gave rise to a shift in the position of the beat frequency. For figure 16d, a 3-mm aperture was used to isolate a single beat signal. The isolation of the beat signal was very good in this case.

There is some doubt as to whether the effects shown in figure 16 are effects caused by the presence of off-axis modes. The strength of these modes was so large that there should be beats between these modes, without the presence of the CO_2 laser radiation. No such beats were seen when the CO_2 was blocked.

If the power of the two lasers which are used in a heterodyne experiment is large, then the photomixer will be driven so hard that harmonics of the beat frequency will be generated. This has been seen in this photomixer using two CO_2 lasers. The relative power levels of the two CO_2 lasers was 1.0 mW and 5.0 μW, which were approximately the same values used in figure 16. Thus, the spikes may in truth be harmonics of the beat frequency.

If lasers have some of their transmitted energy reflected back into the optical cavity, the frequency of the emitted radiation may be changed. Weak modes may be strengthened at the expense of stronger modes. Reflections from the optical elements in the heterodyne system may have returned to the TDL optical cavity and caused the TDL to change frequency slightly. The time variation of the beat signal could have been due to the vibration of the TDL caused by the closed cycle cooler which was used to control the temperature of the TDL. As the aperture was moved around in front of the TDL collection lens, different weak modes were being

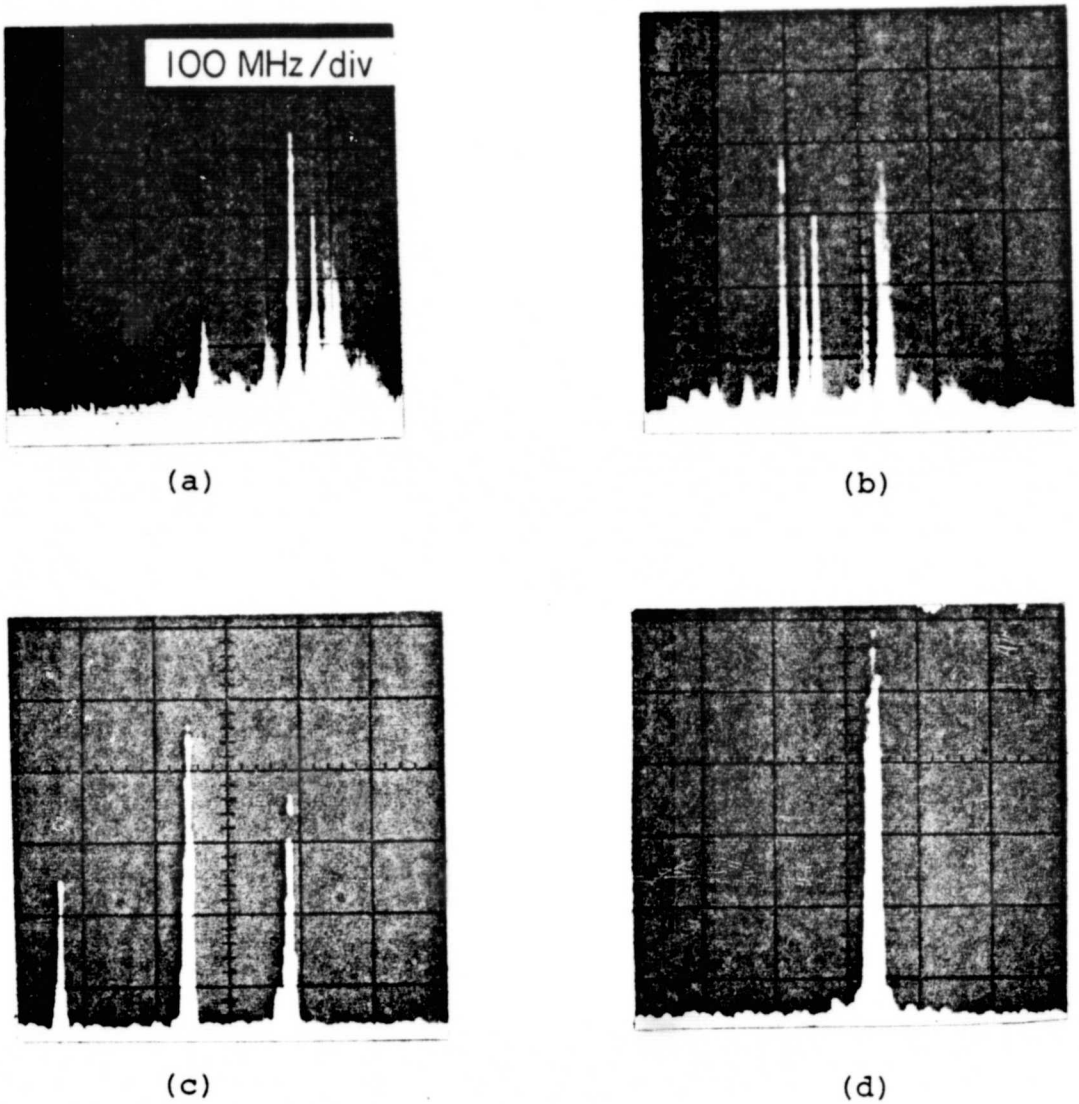

Figure 16. Beat signals. These beat signals were obtained by beating a TDL with a CO_2 laser. The operating conditions were the same in all 4 photographs except that an 8-mm aperature was moved around in front of the TDL collecting lens in the case of (a), (b), and (c); (d) was obtained by placing a 3-mm aperture in front of the lens to isolate a single beat signal.

strengthened. When the similar aperture was used, the feedback to the TDL was minimized.

The exact cause of the effect demonstrated in photographs in figure 16 is not known at the present. Further investigation of the causes of this effect needs to be made, since this effect would be detrimental to the use of the TDL as an LO. However, this phenomenon occurred only once in almost four months of continuous operation of the TDL.

Figure 17 shows the distribution of the power in the TDL line width. This photograph was taken of the beat signal displayed with a logarithmic vertical scale. Each division on the vertical scale represents a 10-dB difference in power level of the signal. The 3 dB points were ~20 MHz apart, but the TDL still had power out to 200 MHz to either side of the peak. However, the power level was down by 30 dB at these frequencies.

The question now arises as to what other factors affect the distribution of power in the TDL emission line. One such factor is demonstrated in figures 18a and 18b These photographs show the beat frequency between the TDL and the CO_2 laser. The operating conditions were the same in each except the closed cycle cooler was turned on in figure 18a and was turned off in figure 18b. The beat frequency was much narrower in figure 18b. The vibrations of the closed cycle cooler caused the TDL emission line width to be much broader when the cooler was on. Figures 19a and 19b show this effect even more graphically. Figure 19a shows the beat signal between the TDL and CO_2 laser. The vertical output of the spectrum analyzer was filtered by a 100-Hz video filter so the effects of the closed cycle cooler could be more readily seen. The horizontal axis scan rate was 2.0 sec/div. The vibration of the closed cycle cooler manifests itself in the spikes and valleys seen in this figure. The closed cycle cooler had a 3.0-Hz frequency, and this was readily discerned from the time variation of the beat signal with 2 or 3 spikes occurring during 1 cycle of the cooler. Accelerometer tests carried out on the cold head of the closed cycle cooler showed multiple bursts of

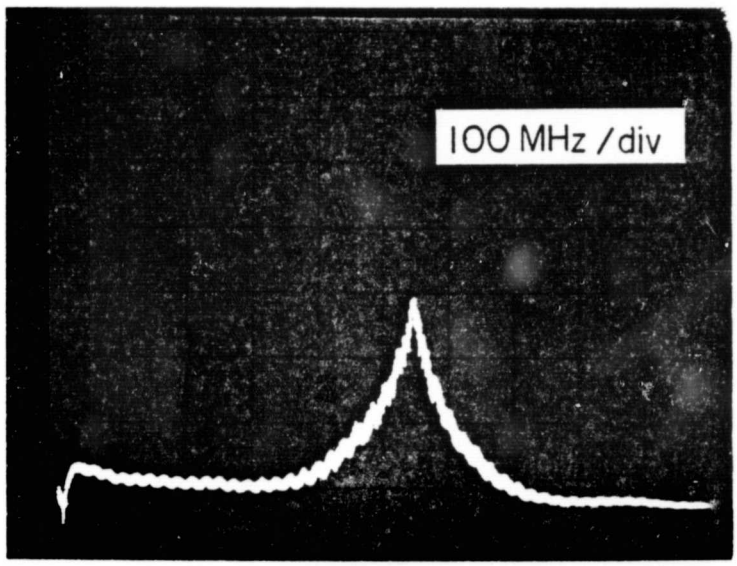

Figure 17. Spectral power distribution of TDL beat signal. The photograph shows the trace from the spectrum analyzer of the beat signal between the CO_2 laser and the TDL. The vertical scale was logarithmic with 10 dB/div with a 10-Hz video filter applied to the output signal. The horizontal scale was 100 MHz/div. The 3-dB halfwidth was approximately 20 MHz. The power in the beat signal extended out to 200 MHz from the center, but it was down by 30 dB at that point. This power distribution is indicative of the power distribution in the TDL line width since the CO_2 line width has been measured previously to be less than 0.1 MHz.

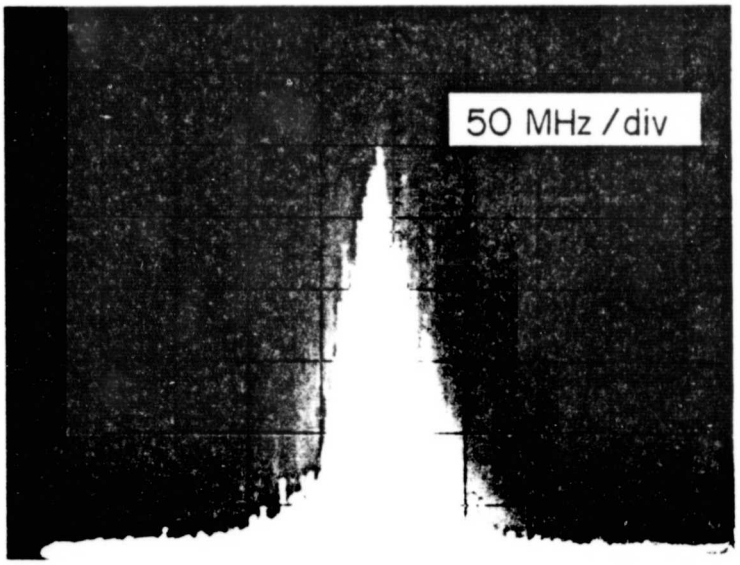

(a)

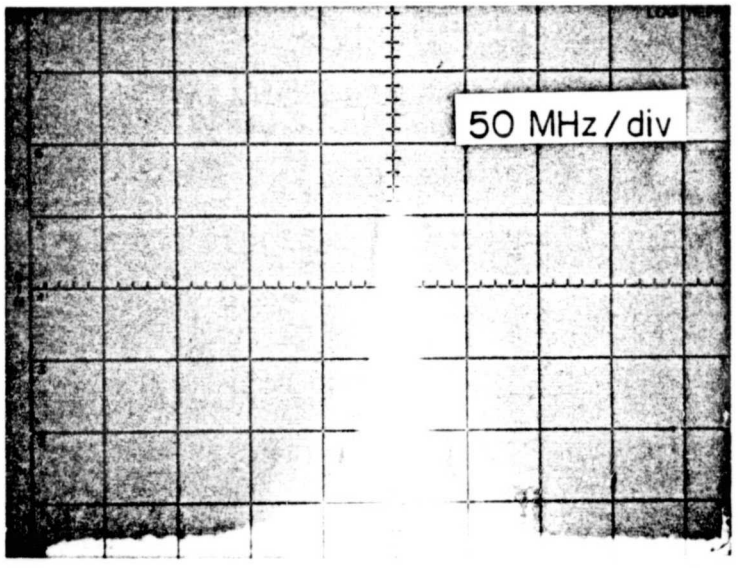

(b)

Figure 18. Beat signal of TDL. These two photographs show the effects of the TDL closed cycle cooler on the beat signal between the TDL and the CO_2 laser. The operating conditions were the same in both photographs, but in (a) the closed cycle cooler was on, and in (b) the cooler was off. The halfwidth of the beat signal was narrower when the closed cycle cooler was off.

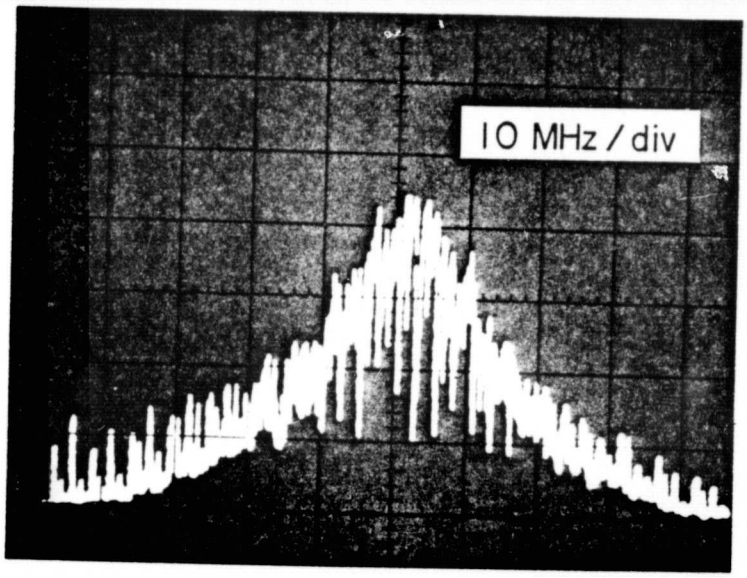

(a)

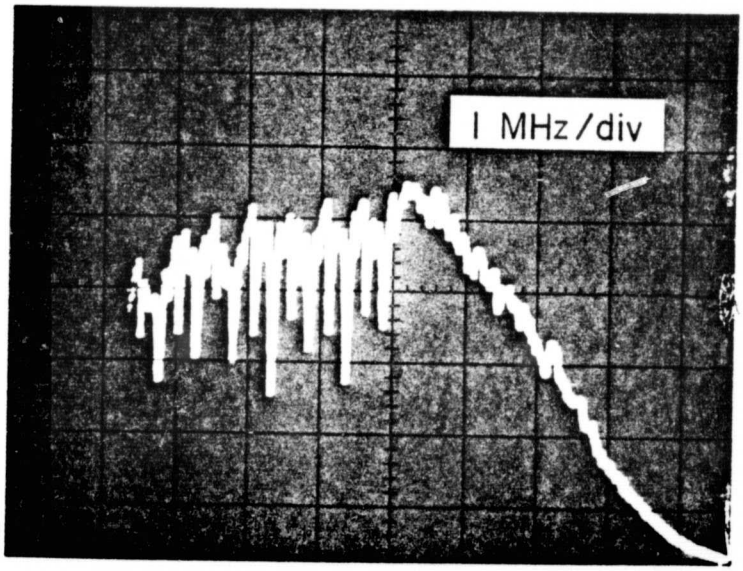

(b)

Figure 19. Beat signal under high resolution. These two photographs show the beat signal between the TDL and CO_2 laser under higher resolution than shown in figures 18(a) and 18(b). The vertical scale in (a) was linear with 100-Hz video filtering. The spikes and depression in (a) are caused by the 3-Hz cycle of the closed cycle cooler, (b) shows the effects of turning off the closed cycle cooler at the center of the beat frequency scan. The disappearance of the depressions on the vertical output coincided with the turning off of the closed cycle cooler.

vibrations during a single cycle. Figure 20b shows the effect of turning off the closed cycle cooler at the middle of the frequency scan. The scan rate was 0.5 sec/div, and a 10-Hz video filter was connected to the vertical axis. The disappearance of the spikes and valley at the center of the photograph marks the point where the closed cycle cooler was turned off. The drop in the level of the beat signal was due to the temperature tuning of the TDL caused by a temperature rise at the cold head of the cooler. If the TDL were mechanically isolated from these vibrations, its line width would be much narrower than presently possible. Even with the vibration problems, beat signals with 10 MHz halfwidths have been measured. One such beat signal is shown in figure 20. Thus, if a vibration isolation system can be designed, the TDL line width will be narrower.

III. Comparison of TDL and CO_2 Local Oscillators

In order to compare the TDL with the CO_2 laser as local oscillators, the TDL was used as an LO in the heterodyne system shown in figure 3. Here the CO_2 laser in figure 3 was replaced by a 1500° C black body (BB) and a lens, which was used to match the radiation from the BB to the antenna pattern of the heterodyne system with the TDL as the LO. An 8.0-μm to 14-μm bandpass optical filter was used to reduce the amount of BB radiation which was outside the heterodyne system's bandwidth. A mechanical chopper was also placed in the BB leg of the system and was used so that the BB IF beat signal along with the noise could be measured with a lock-in amplifier.

When the TDL current is increased, the emission frequency is changed. Figure 21 shows the heterodyne signal as the TDL current was changed. Figure 21 shows the scan from 0.75 to 2.0 amps. The change in the noise level at 1.25 amps was caused by a change in the time constant. The heterodyne signal steadily increased over the scan. The time constant was 0.4 sec with a 12 dB/octave rolloff. The signal-to-noise level was ~15 around 1.75 amps. With additional filtering and a decrease of the scan rate, this beat signal could be used to measure spectra of an absorbing gas placed in the BB path even though the TDL power level was only 30 μW. The noise level in figure 21 increased significantly at 1.75 amps and beyond. IF spectra are shown in figures 22a, 22b, and 22c, when the TDL was operating at a current beyond 1.75 amps. These IF spectra are typical when excessive noise appeared on the heterodyne signal. This broad band noise has been attributed to competition between modes of the TDL. This was supported by wavelength scans of the TDL emission taken at different TDL current settings. These spectra are shown in figure 23. They were taken with the 0.5-meter spectrometer shown in figure 3 with a slit setting of 200 μm. All of these spectra showed well separated modes for currents below 1.8 amps. The spectra for currents 1.8 amps and above showed one or more small modes, and the mode spectra were not as well separated as previously. The presence of these small modes

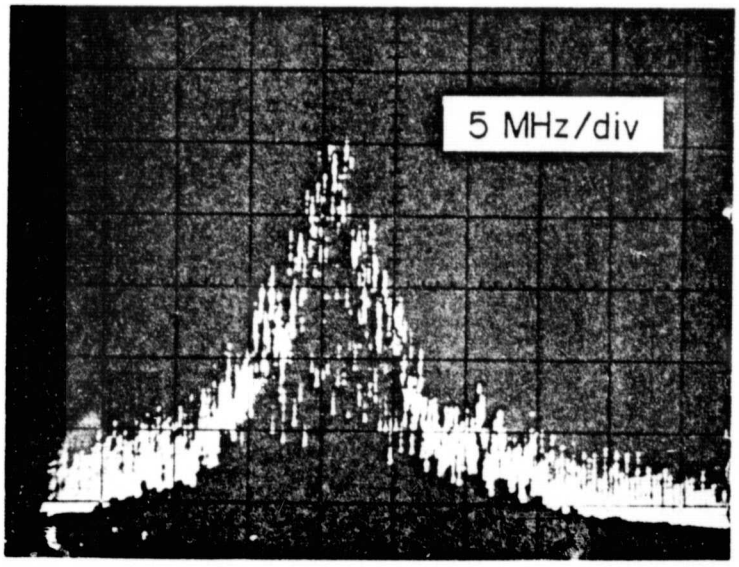

Figure 20. Best beat signal. This photograph shows the narrowest beat signal obtained during the course of this research. A 100-Hz video filter was applied to the vertical linear scale. The horizontal scale was 5 MHz/div. The halfwidth was 10 MHz. The effects of the cooler on the output trace were evident.

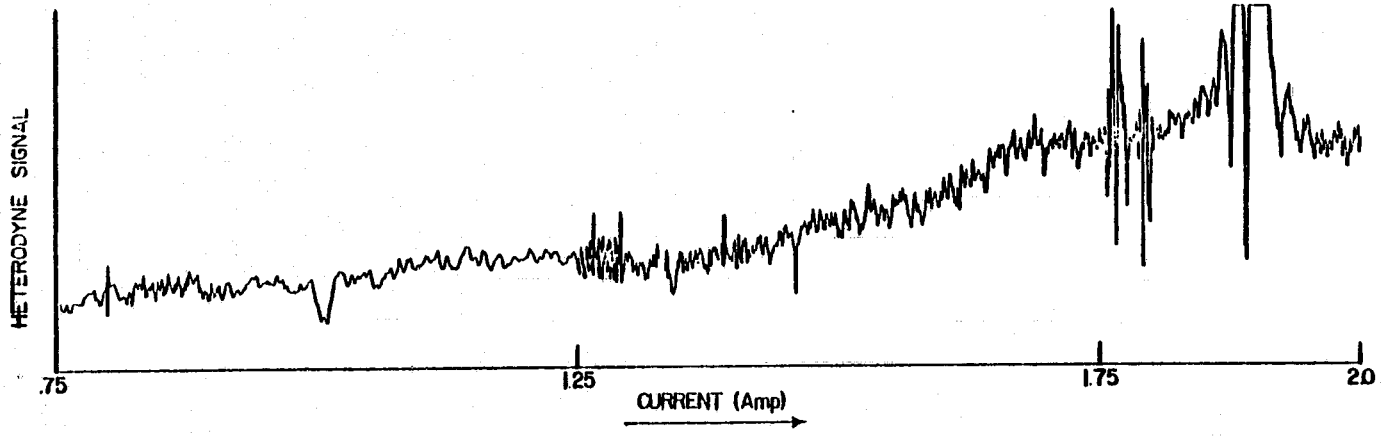

Figure 21. Black body heterodyne signal with TDL local oscillator. This figure shows the heterodyne signal obtained by beating the TDL against a 1500°C black body as a function of the TDL current. The change in the noise level at 1.25 amps corresponds to a change in the time constant of the system. The noise region beyond 1.75 amps was due to excess RF noise generated by the TDL. This excess noise has been attributed to mode competition in the TDL. The TDL power on the photomixer was ~30 μW when the heterodyne signal was the largest.

in the mode spectra were usually an indicator that excess noise would appear on the heterodyne signal.

One important point needs to be made. Although the excess noise does appear to be a problem in the heterodyne process, the percentage of the useful TDL tuning range that gives a good heterodyne signal is quite large. This is a tremendous improvement over the previously published work of Ku and Spears (ref. 11), where the excessively noisy regions took up the major portion of the TDL tuning range.

In the subsequent black body heating experiment, 60 μW of multi-mode TDL power was focused on the photomixer and mixed with the radiation from a 1000° C BB. This gave a signal-to-noise ratio of 23. When the TDL was replaced by the CO_2 laser, a signal-to-noise ratio of 44 was obtained from the same CO_2 power level. Thus, the CO_2 laser was only a factor of 1.9 better than the TDL. Hence, if the power level of the TDL were increased, the TDL would make an excellent LO for heterodyne measurement.

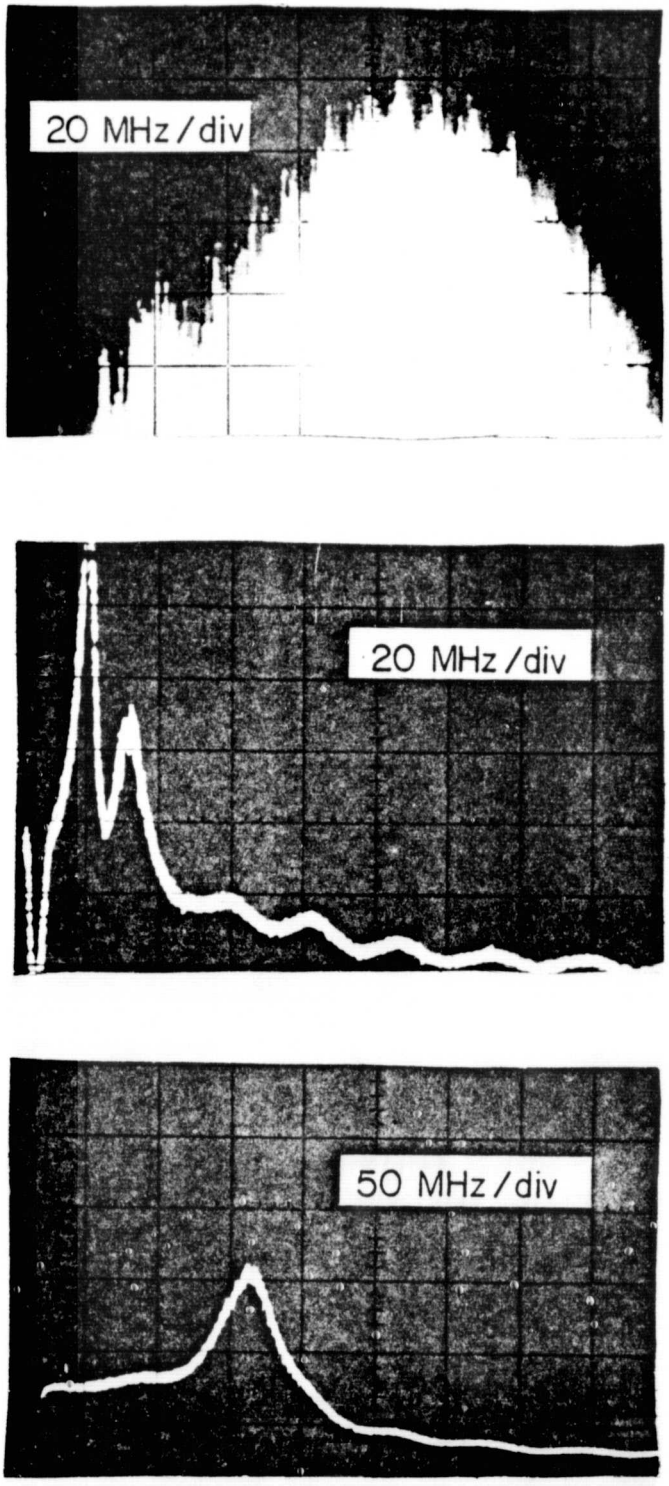

Figure 22. RF spectra of excess noise in TDL. These three photographs show the output of the spectrum analyzer when the TDL was operating such that excessive noise appeared on the black body heterodyne signal.

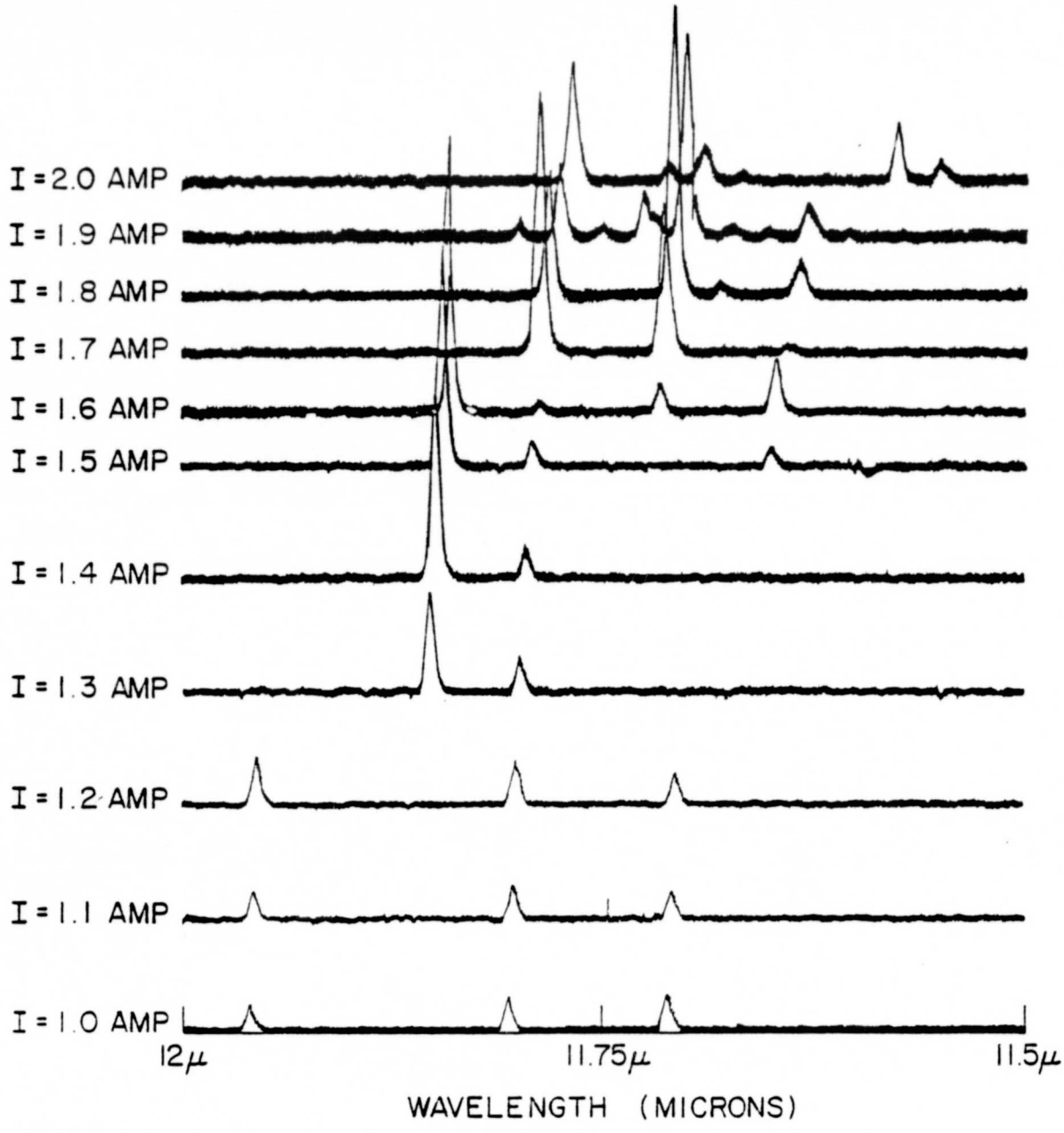

Figure 23. Mode spectra of TDL. These curves show the spectra obtained by scanning a 0.5-meter spectrometer over the TDL emission for the same temperature and current settings used to generate figure 22. The modes of the TDL were well separated for TDL currents below 1.80 amps; above this several smaller modes appear. Competition between these modes is thought to have caused the excessive noise seen on figure 21. This type of mode structure was seen for all mode scans where the TDL was operating at conditions which gave rise to the excessive RF noise.

RESULTS AND CONCLUSIONS

A HgCdTe photomixer heterodyne system has been analyzed by a new method which showed that the heterodyne response as a function of beat frequency has a rolloff that is much different from the rolloff obtained from the shot noise measurements,i.e. 100 MHz compared to 1000 MHz. These results are consistent with the results of Spears (ref. 8).

The signal-to-noise ratio obtained with a CO_2 laser beating against a 1000° C black body gave a signal-to-noise ratio which was only a factor of 1.76 from the theoretical calculations with the effects of shot noise, amplifier noise, Johnson noise, and dark current noise included with an assumed IF bandwidth of 1.0 GHZ. If a bandwidth of 322 MHz was assumed, the theoretical and experimental results agree. This bandwidth was more consistent with the TDL heterodyne response curves.

The evaluation of this single and other photomixers (ref. 12) indicates that the heterodyne response of a photomixer heterodyne system is sufficiently different from the conventional low frequency measurements that the frequency response must be checked out independently. If the correct frequency response of the photomixer system is used, then theory and experiment will be in better agreement.

The TDL evaluation showed that a heterodyne system can use a TDL as an LO, even with the low power which is available from the TDL; usable signal-to-noise ratios can be obtained which are within a factor of 1.9 from that obtained with a CO_2 laser operating with the same power level. The tuning range of TDL which is useful for heterodyne operation has improved over previously published results.

The state of the art in the production of TDL has improved significantly in the past years. Since the completion of this evaluation, the state of the art has improved to such an extent that TDL's have been produced which have power levels between 1.0 to 2.0 mW. When these lasers are evaluated, there will surely be a tremendous improvement in the heterodyne system's response with the TDL as the LO.

REFERENCES

1. Menzies, R.T. and M.S. Shumate: Air Pollution: Remote Detection of Several Pollutant Gases with a Laser Heterodyne Radiometer. Science, Vol. 184, 570, 1974.

2. Menzies, R.T. and M.T. Chakine: Remote Atmospheric Sensing with an Airborne Laser Absorption Spectrometer. Applied Optics, Vol. 13, 2840, 1974.

3. Menzies, R.T. and M.S. Shumate: Remote Measurements of Ambient Air Pollutants with a Bistatic Laser System. Applied Optics, Vol. 15, 2080, 1976.

4. Seals, R.K. and B.J. Peyton: Remote Sensing of Atmospheric Pollutant Gases Using an Infrared Heterodyne Spectrometer. Proceedings of the International Conference on Environmental Sensing and Assessment, Vol. 1, September 1975, Las Vegas, Nevada.

5. Peyton, B.J., R.A. Lange, M.G. Savage, R.K. Seals, and F. Allario: Infrared Heterodyne Spectrometer Measurements of Vertical Profile of Tropospheric Ammonia and Ozone. AIAA 15th Aerospace Sciences Meeting, January 24-26, 1977, Los Angeles, California.

6. Mumma, M.M. and T. Kostiuk: Infrared Heterodyne Spectroscopy of Astronomical and Laboratory Sources at 8.5 μm. Nature, 253, 514, 1975.

7. Ferking, M.A.: Infrared Heterodyne Spectroscopy of Atmospheric Ozone. IEEE/OSA Conference on Laser Engineering and Applications, June 1-3, 1977, Washington, DC.

8. Spears, D.L.: Heterodyne Sensitivity Evaluation of GHz Bandwidth 10.6 μm Photodiodes. Proceedings of the IRIS Detector Specialty Group Meeting, March 22-23, 1977, U.S. Air Force Academy, Colorado.

9. Abbas, M.M., M.M. Mumma, T. Kostiuk, and D. Buhl: Sensitivity Limits of an Infrared Heterodyne Spectrometer for Astrophysical Applications. Applied Optics, Vol. 15, 427, 1976.

10. Siegman, A.E.: The Antenna Properties of Optical Heterodyne Receivers. Proceedings of the IEEE, Vol. 54, 1350, 1966.

11. Ku, R.T. and D.L. Spears: High-Sensitivity Heterodyne Radiometer Using a Tunable Diode Laser Local Oscillator. 1977 IEEE/OSA Conference on Laser Engineering and Applications, June 1-3, 1977, Washington, DC.

12. To be published.